Atmos. Chem. Phys., 9, 8351–8363, 2009
www.atmos-chem-phys.net/9/8351/2009/

Atmospheric Chemistry and Physics

Toward a general parameterization of N_2O_5 reactivity on aqueous particles: the competing effects of particle liquid water, nitrate and chloride

T. H. Bertram[1,*] **and J. A. Thornton**[1]

[1]Department of Atmospheric Sciences, University of Washington, Seattle, WA, USA
[*]now at: Department of Chemistry, University of California San Diego, La Jolla, CA

Received: 12 June 2009 – Published in Atmos. Chem. Phys. Discuss.: 14 July 2009
Revised: 2 October 2009 – Accepted: 5 October 2009 – Published: 3 November 2009

Abstract. The heterogeneous reaction of N_2O_5 on mixed organic-inorganic aerosol particles was investigated using an entrained aerosol flow tube coupled to a custom-built chemical ionization mass spectrometer. Laboratory results on aqueous particles confirm a strong dependence of the reactive uptake coefficient (γ) on particle liquid water, for particle water concentrations below 15 M, and the molar ratio of particle water to nitrate. Measurements of $\gamma(N_2O_5)$ on mixed chloride-nitrate particles indicate that the presence of trace chloride can negate the suppression of $\gamma(N_2O_5)$ at high nitrate loadings with implications for polluted coastal regions. These results are used to construct a new parameterization for $\gamma(N_2O_5)$, that when coupled to an aerosol thermodynamics model, can be used within regional and/or global chemical transport models.

1 Introduction

The heterogeneous reaction of dinitrogen pentoxide (N_2O_5) on aerosol particles plays a critical role in regulating tropospheric reactive nitrogen ($NO_x \equiv NO + NO_2$) availability (Dentener and Crutzen, 1993), contributes to particulate nitrate (NO_3^-) loadings (Riemer et al., 2003) and promotes halogen activation following reaction on chloride containing particles (Behnke et al., 1997; Finlayson-Pitts et al., 1989; Osthoff et al., 2008; Thornton and Abbatt, 2005). The efficiency with which N_2O_5 reacts on particles is expressed as a reaction probability (γ), defined as the fraction of gas-particle collisions that result in net removal of N_2O_5 from the gas-phase. Early laboratory measurements demonstrated that N_2O_5 reacts readily on cold acidic particles ($\gamma(N_2O_5) = 0.1$), characteristic of the chemically uniform sulfuric acid (H_2SO_4) particles present in the stratosphere (Fried et al., 1994; Mozurkewich and Calvert, 1988). Using a global chemical transport model, Dentener and Crutzen applied these measurement constraints (i.e., $\gamma(N_2O_5) = 0.1$) to the troposphere, where particle surface area concentrations (S_a) can be a factor of 50 higher, finding that 50% of NO_x emissions are removed via N_2O_5 heterogeneous reactions as a global, annual average (Dentener and Crutzen, 1993). However, in contrast to the uniform chemical composition of stratospheric particles, tropospheric particles are chemically diverse and strong variations in ambient relative humidity (RH) lead to varying levels of particle liquid water. As a result, strong variations in $\gamma(N_2O_5)$ are expected and have been confirmed by laboratory investigations (Anttila et al., 2006; Cosman et al., 2008; Folkers et al., 2003; Hallquist et al., 2003; Kane et al., 2001; Knopf et al., 2007; McNeill et al., 2006; Mozurkewich and Calvert, 1988; Park et al., 2007; Thornton and Abbatt, 2005; Thornton et al., 2003) and measurements of the steady-state lifetime of N_2O_5 (Brown et al., 2006). Results from these studies have been used to refine the parameterization of $\gamma(N_2O_5)$ in the current generation of regional and global models (Davis et al., 2008; Evans and Jacob, 2005; Riemer et al., 2003).

A limitation of most previous laboratory experiments is that they were performed using single component condensed phases. In contrast, most tropospheric particles are a mixture of multiple components (Murphy et al., 2006). Here, we build upon the existing set of laboratory investigations of $\gamma(N_2O_5)$, by directly probing the competing effects of

Correspondence to: J. A. Thornton
(thornton@atmos.washington.edu)

particle liquid water content (H_2O(l)), nitrate (NO_3^-) and chloride (Cl^-) using internally mixed particles representative of the lower troposphere. We report $\gamma(N_2O_5)$ for a series of mixed inorganic and organic aerosol particles over a wide range in H_2O(l). These new measurements help test current mechanistic theories of N_2O_5 reactivity in aqueous solutions and thus aid the development of a more chemically accurate parameterization for $\gamma(N_2O_5)$ that, when coupled to an aerosol thermodynamics model, can be used in chemical transport models.

2 Experimental design

2.1 The N_2O_5 reaction mechanism in aqueous solutions

Our experimental design was based on testing the currently accepted mechanism for the reaction of N_2O_5 on aqueous solution particles. The concerted reaction mechanism for the hydrolysis of N_2O_5 on mildly acidic to near neutral particles, characteristic of the troposphere, has been summarized by Thornton et al. (2003). The reaction is initiated by mass accommodation (α) to the particle surface (R1), forming aqueous phase N_2O_5 that reacts reversibly with liquid water to form a protonated nitric acid intermediate ($H_2ONO_2^+$) Reaction (R2). We note that $H_2ONO_2^+$, functionally equivalent to invoking a solvated NO_2^+ or a solvated N_2O_5 with high ionic character, has never been directly observed in the systems discussed here, and is thus only a construct with which to interpret the observed N_2O_5 reactivity and products. In pure water, $H_2ONO_2^+$ will proceed to react with H_2O(l) forming aqueous nitric acid (HNO_3) (R3). In the presence of stronger nucleophiles, such as halide ions, the reaction can result in nitryl halide formation: XNO_2 (where X = Cl, Br, or I) (Behnke et al., 1997; Finlayson-Pitts et al., 1989; Schweitzer et al., 1998; Thornton and Abbatt, 2005).

$$N_2O_5(\text{gas}) \xleftrightarrow{k_1} N_2O_5(aq) \quad \text{(R1)}$$

$$N_2O_5(aq) + H_2O(l) \xrightarrow{k_{2f}} H_2ONO_2{}^+(aq) + NO_3{}^-(aq) \quad \text{(R2)}$$

$$H_2ONO_2{}^+(aq) + NO_3^-(aq) \xrightarrow{k_{2b}} N_2O_5(aq) + H_2O(l)$$

$$H_2ONO_2{}^+(aq) + H_2O(l) \xrightarrow{k_3} H_3O^+(aq) + HNO_3(aq) \quad \text{(R3)}$$

$$H_2ONO_2^+(aq) + X^- \xrightarrow{k_4} XNO_2 + H_2O(l) \quad \text{(R4)}$$

The proposed reaction mechanism qualitatively explains the dependence of $\gamma(N_2O_5)$ on: i) H_2O(l) (Thornton et al., 2003), ii) particle NO_3^-, which inhibits N_2O_5 hydrolysis (R2) (Mentel et al., 1999; Wahner et al., 1998), and iii) organic coatings, which have been theorized to either suppress N_2O_5 accommodation Reaction (R1) or decrease water availability at the surface (Anttila et al., 2006; Cosman et al., 2008; Folkers et al., 2003; Knopf et al., 2007; McNeill et al., 2006; Park et al., 2007). Highly acidic particles, such as those found in the stratosphere or in ammonia-deficient regions of the troposphere, appear to promote an additional acid catalyzed channel, with $\gamma(N_2O_5)$ measured on such particles to be between 0.03–0.1 and thus not necessarily consistent with the above mechanism (Fried et al., 1994; Hu and Abbatt, 1997; Mozurkewich and Calvert, 1988; Robinson et al., 1997).

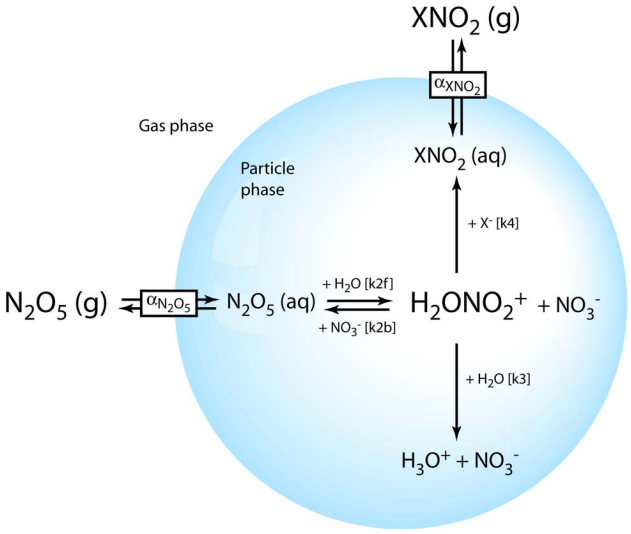

Fig. 1. Schematic depiction of the heterogeneous reaction of N_2O_5 with aerosol particles. Following accommodation ($\alpha_{N_2O_5}$) to the particle, aqueous N_2O_5 dissociates into the reactive intermediate $H_2ONO_2^+$, which can proceed either through reaction with H_2O or X^- to promote N_2O_5 reactivity, or recombine with NO_3^- to suppress net reactivity.

In this study, we test this proposed reaction mechanism concentrating on the fate of the reaction intermediate $H_2ONO_2^+$ as the principle driver for net N_2O_5 reactivity in aqueous solutions. As shown in Reactions (R1–4) and Fig. 1, $H_2ONO_2^+$ reacts either with H_2O, NO_3^- or X^-, where only reactions with NO_3^- impede net N_2O_5 reaction. Within this reaction framework, $\gamma(N_2O_5)$ depends on particle H_2O(l), NO_3^- and X^- abundance, and their corresponding liquid phase reactions rate coefficients (k_2-k_4).

2.2 Experimental apparatus

We use an entrained aerosol flow tube coupled to a custom-built chemical ionization mass spectrometer (CIMS) to directly determine the pseudo-first order rate coefficient (k_{het}) for the heterogeneous reaction of N_2O_5 on aerosol particles. The experimental approach is similar to that described in detail in Thornton et al. (2003). In the following, we

briefly describe the experiment, highlighting changes to the approach of Thornton et al. (2003).

2.2.1 Aerosol generation, conditioning and characterization

Aerosol particles were generated from aqueous solutions of mixed organic and inorganic components (0.05–0.1 wt%) using a constant output atomizer (TSI Inc., Model 3076). Ammonium bisulfate (Alfa Aesar, 99.9%), malonic acid (Sigma Aldrich, >98%), NaCl (J. T. Baker, >99%), and $NaNO_3$ (J. T. Baker, >99%) were used without further purification and diluted into de-ionized or millipure water (resistivity >18 MΩ cm). The purity and composition of each atomizer solution was then independently checked by ion chromatography (IonPac AS11 Anion-Exchange Column, Dionex Corporation). In this regard, a trace impurity (0.1%) of NaCl was noted in the $NaNO_3$ stock used, and we adjusted our predicted particle compositions accordingly.

Aerosol particles from the atomizer were conditioned to the desired relative humidity by mixing the atomizer output with N_2 at the appropriate RH. The RH was measured in both the particle delivery line and the flow reactor using a commercial hygrometer (Vaisala), achieving an accuracy of ±2%. Following equilibration, the mixed flow was either sampled directly into the flow reactor for N_2O_5 decay determinations as in Thornton et al. (Thornton et al., 2003), or directed through a two-state filter manifold system designed to modulate the flow direction between filter-inline and filter-bypassed states for calculation of the N_2O_5 loss rate via the approach described in Bertram et al. (2009). The filter manifold permitted measurements to be conducted in the presence or absence of particles while maintaining nearly constant RH, a key requirement for assessing the contribution of N_2O_5 wall losses to the observed loss of N_2O_5 in the presence of particles (see Sect. 2.5).

Particle size distributions (10–800 nm) were measured continuously using a differential mobility analyzer (DMA) coupled to an ultra-fine condensation particle counter (Grimm Technologies). Particle surface area concentrations ranged between $0.2–2.0\times10^{-3}$ cm^2 cm^{-3}, while the mean surface area weighted particle diameter ranged between 150–200 nm, depending on RH and the wt % of solutes in the atomizer solution. Size distributions measured in this study were similar to those shown in Thornton et al. (2003) for 0.1 wt% malonic acid solutions, where extrapolation of the size distribution beyond 800 nm accounts for less than 5% of additional particle S_a. The DMA sheath flow was made up from the humidified sample flow eluting from the flow reactor, and was allowed to equilibrate with the sample RH prior to measuring the particle size distributions. Thus, particle size distributions measured by the DMA are reflective of those in the flow reactor.

Particle liquid water and aqueous phase particle inorganic and organic mole fractions were calculated for each experiment using the online version of the aerosol inorganics model (AIM Model II, http://www.aim.env.uea.ac.uk/aim/aim.php) which can be compiled to include the effects of specific organics on H_2O(l) (Carslaw et al., 1995, Clegg et al., 1998, Wexler and Clegg, 2002). Particle liquid water concentration was then calculated from the AIM output and the respective densities of the chemical constituents, where the calculated particle densities ranged between of 1.25 and 2 g cm^{-3}. The measured RH in the flow tube and the concentrations of solutes in the atomizer solutions were used as inputs for the model. The AIM model was run with suppressed crystallization as the RH in the flow reactor was always held above the efflorescence RH for each individual component and the particles were initially aqueous at the atomizer output.

2.2.2 N_2O_5 synthesis

The N_2O_5 source is described in detail in Bertram et al. (2009). Briefly, N_2O_5 was generated in situ from the reaction of ozone (O_3) with nitrogen dioxide (NO_2) and subsequent reaction of the nitrate radical product (NO_3) with NO_2. Trace O_3, generated via photolysis of oxygen at 185 nm, was mixed with excess NO_2 (Scot Marin specialty gases) and permitted to react for two minutes. The N_2O_5/NO_3 ratio was greater than 100 at room temperature (298 K) due to excess NO_2 that chemically shifts the equilibrium in favor of N_2O_5. Following a 10:1 dilution into the flow reactor, the typical initial concentrations of N_2O_5, NO_3, O_3 and NO_2 at the top of the flow tube were 5 ppbv (1.2×10^{11} molecules cm^{-3}), 50 pptv (1.2×10^{9} molecules cm^{-3}), 20 ppbv (4.9×10^{11} molecules cm^{-3}), and 100 ppbv (2.4×10^{12} molecules cm^{-3}), respectively.

2.2.3 Entrained aerosol flow reactor

The ambient pressure flow reactor used in the following experiments is a 3 cm ID, vertically oriented, halocarbon coated (Halocarbon Inc. Series 1500) pyrex tube, 90 cm in length. Particles are introduced into the flow reactor via a sidearm orientated orthogonal to the flow direction of the reactor. Gas-phase reactants and products and particle size distributions were monitored at the base of the flow reactor via the CIMS and DMA/CPC, respectively. Routine measurement of the particle size distribution at the flow reactor entrance confirmed that particle surface area transmission was greater than 90%. The flow velocity through the reactor is set by the combined flow rate of the CIMS (1.5 slpm) and DMA/CPC (0.3 slpm). The resulting linear flow velocity was 4.25 cm s^{-1}, leading to fully developed laminar flow within 15 cm downstream of the introduction of the aerosol flow to the reactor (Kay and Nedderman, 1985).

N_2O_5 was added to the flow reactor via a 3 mm OD PFA tube, housed in a 6 mm OD stainless steel moveable injector, inserted axially down the center of the flow reactor (McNeill et al., 2006). The time required for complete mixing of the injected N_2O_5 flow (0.1 slpm) with the aerosol-laden bulk flow stream (1.7 slpm) is controlled by the gas-phase diffusion constant for N_2O_5, which when taken to be 0.1 $cm^2\ s^{-1}$ (Hu and Abbatt, 1997), yields an estimated mixing time of 4.5 s or 19 cm. To ensure that the reaction was probed under fully developed laminar flow conditions and that N_2O_5 had mixed completely with the bulk aerosol flow stream, we use the central 50 cm of the flow reactor to probe the gas-particle reaction.

2.2.4 CIMS detection of N_2O_5 and $ClNO_2$

N_2O_5 and $ClNO_2$ were detected directly by CIMS at the base of the flow reactor following the approach of Kercher et al. (2009). Iodide ions (I^-), produced by passing trace methyl iodide (CH_3I) in N_2 over a ^{210}Po ion source (NRD Inc., P-2021 inline ionizer), were used as the reagent ions for the sensitive (>1 Hz $pptv^{-1}$) specific detection of N_2O_5 and $ClNO_2$ at 234.9 amu ($I^- \times N_2O_5$) and 207.9 amu ($I^- \times ClNO_2$), respectively. The low detection thresholds achieved by the CIMS (<5 pptv in 60 s) permit experiments to be conducted at atmospherically relevant mixing ratios, so as to minimize the impact of NO_3^- accumulation in the particle which can artificially suppress reactivity. The specificity of the $I^- \times N_2O_5$ detection scheme over detection at 62 amu (NO_3^-) eliminates potential interferences from HNO_3 in the flow reactor, commonly observed at 62 amu in the presence of O_3.

2.3 Determination of k_{het} and $\gamma(N_2O_5)$

First-order rate coefficients (k_{obs}) were determined by one of two methods. In the first method, the decay in the concentration of N_2O_5 was observed as a function of gas-particle interaction times (Δt) by varying the position of the moveable injector. The slope of the uncertainty-weighted linear least squares fit to the natural log of N_2O_5 versus Δt yielded k_{obs}. Decays were performed in the presence and absence of particles to determine the wall loss corrected first-order rate coefficient for loss to particles only (k_{het}). Corrections due to non-plug flow conditions and incorporation of the first-order rate coefficient for loss to the reactor walls (k_{wall}) were made using the standard iterative approach designed by Brown et al. (1978). Corrections due to non-plug flow conditions resulted in a 10–15% increase in k_{het} over the uncorrected values. While this method has been proven robust and provides direct information on the reaction order, it necessitates that the particle surface area concentration and RH remain constant over the course of a full decay (several minutes). This requirement is often difficult to achieve due to variations in the atomizer output that result in variations in S_a of order 10–20% on the time-scale of a single decay. In addition, the decay method is sufficiently labor intensive due to the requirement of measuring full decays in the presence and absence of particles at each reaction condition.

Given the challenges of the decay method, we also used the particle modulation technique developed previously as described by Bertram et al. (2009) for k_{het} determinations. If the particle and wall reactions are first order in N_2O_5, as is the case for the reactions studied here, k_{het} can be calculated from Δt and the measured mixing ratio of N_2O_5 in the presence ($[N_2O_5]_{w/aerosol}$) and absence of particles ($[N_2O_5]_{wo/aerosol}$).

$$k_{het} = -\left(\frac{1}{\Delta t}\right)\ln\left(\frac{[N_2O_5]^{w/particles}_{\Delta t}}{[N_2O_5]^{wo/particles}_{\Delta t}}\right) \quad (1)$$

This alternative approach allows us to rapidly toggle between particle-present and particle-absent states to quickly build a series of independent determinations of k_{het} and thus to reduce the uncertainty associated with fluctuations in RH and S_a. In this method, we fix the injector position at 70 cm, corresponding to a Δt of 17 s and subtract the time required for mixing (~4 s), resulting in a lower limit estimate for Δt. The Brown et al. (1978) correction for non-plug flow conditions requires a simultaneous estimate of k_{wall} which is not available from this method. Thus, we apply correction factors obtained from analyzing full decays, as described above, which were made at similar RH values and thus k_{wall}. In any case, these corrections are small, of order 10%, and thus contribute little to the k_{het} values reported here.

The reaction probability is then calculated from the measured k_{het}, determined from either method, using co-located observations of S_a:

$$\frac{1}{\gamma} = \frac{\omega S_a}{4k_{het}} - \frac{0.75+0.283K_n}{K_n(1+K_n)}, \quad (2)$$

where $K_n = \frac{3D_g}{\omega \overline{r_s}}$, $\overline{r_s} = r_p \exp\left(2.5\ (\ln\sigma)^2\right)$

D_g is the gas-phase diffusion coefficient ($cm^2\ s^{-1}$) for N_2O_5, ω is the molecular velocity for N_2O_5 and r_p and $\ln\sigma$ describe the radius and width of the log-normal particle size distribution, respectively (Fuchs and Sutugin, 1970; Hanson and Kosciuch, 2003).

The two retrieval methods, time-dependent decay and particle modulation, were directly compared using aqueous ammonium bisulfate (NH_4HSO_4) at 50% RH. The mean and standard deviation of five independent determinations of $\gamma(N_2O_5)$ using the decay and modulation techniques were 0.031±0.003 and 0.026±0.005 respectively. These results provide confidence that both methods are capable of capturing $\gamma(N_2O_5)$ within the overlap of their combined uncertainty.

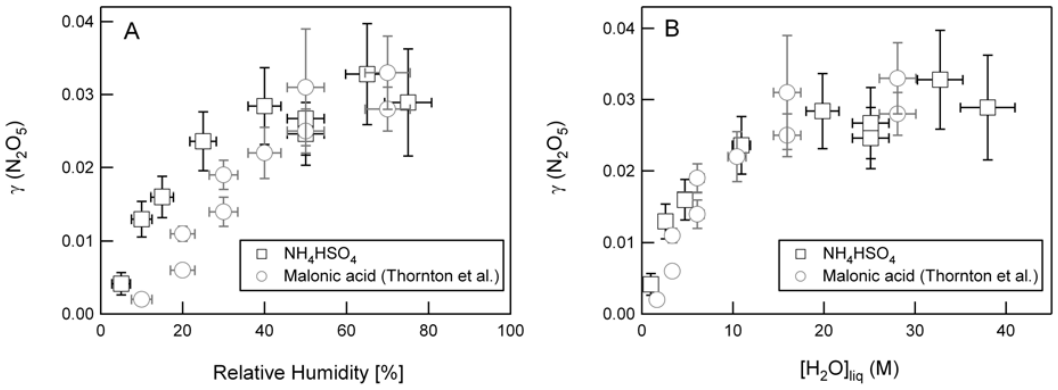

Fig. 2. Dependence of $\gamma(N_2O_5)$ on relative humidity **(A)** and particle liquid water content **(B)** as calculated with the aerosol inorganics model (AIM). Measurements on aqueous NH_4HSO_4 (black squares) are from this study, while observations on malonic acid (gray circles) are from those reported in Thornton et al. (2003). Each individual point in the NH_4HSO_4 dataset represents the mean of five independent measurements and the error depicts the standard deviation in the mean. The x-axis error-bar in panel A depicts the range in RH sampled during the five determinations and that uncertainty is propagated through the calculation of H_2O(l) to give the x-axis error in panel B.

3 Laboratory results and discussion

Results for all of the experiments conducted are summarized in Table 1, where we report the relative humidity measured in the flow reactor, the wt % for all chemical species dissolved in the atomizer solution, and the mean and 1σ values of five independent determinations of $\gamma(N_2O_5)$ acquired using the particle modulation technique.

3.1 Dependence of $\gamma(N_2O_5)$ on H_2O(l)

The dependence of $\gamma(N_2O_5)$ on H_2O(l) was investigated using aqueous NH_4HSO_4 particles. This permitted the analysis of $\gamma(N_2O_5)$ over a wide range of H_2O(l), as efflorescence of NH_4HSO_4 particles has not been observed in the laboratory (Cziczo et al., 1997). The results are compared with those obtained on aqueous malonic acid particles, reported by Thornton et al. (2003), both as a function of RH and H_2O(l), Fig. 2a and b, respectively. Each point for NH_4HSO_4 particles is the mean of five independent observations and the associated error-bar represents the standard deviation of the mean. The x-axis error-bar describes the range in RH for which the observations were taken.

The results indicate a strong dependence of $\gamma(N_2O_5)$ on RH below 50%, as previously observed in the Thornton et al. study (2003). The functional dependence of $\gamma(N_2O_5)$ on RH is slightly different for NH_4HSO_4 as compared to malonic acid, due to possible differences in the hygroscopicity and the non-ideality of water in the resulting solutions (Braban and Abbatt, 2004; Cziczo et al., 1997). In contrast, when plotted as a function of particle water molarity, as determined by AIM, the dependence of $\gamma(N_2O_5)$ on H_2O(l) is independent of particle chemical composition (Fig. 2b) within the 1σ experimental uncertainty. This result indicates that an H_2O limitation is present in either Reaction (R2) or (R3), or that mass accommodation of N_2O_5 is H_2O-dependent. As shown in Fig. 2b, $\gamma(N_2O_5)$ is strongly water limited for H_2O(l) below 15 M; above 15 M there is sufficient H_2O(l) and $\gamma(N_2O_5)$ plateaus at a value of 0.03.

It is important to note that the observed water limitation is not due to an artificial nitrate effect. Neither the addition of N_2O_5 to the flow reactor nor gas-phase HNO_3 partitioning provides enough particulate NO_3^- to induce a nitrate effect in these experiments. We determined the particulate nitrate for the former source by mass balance of the N_2O_5 loss to the particles and for the latter source by monitoring the mixing ratio of HNO_3 in the flow reactor and assuming the gas and condensed phases are in equilibrium.

To the best of our knowledge, there are five previous investigations of the dependence of $\gamma(N_2O_5)$ on RH for aqueous, non-sulfuric acid particles (Folkers et al., 2003; Hallquist et al., 2003; Hu and Abbatt, 1997; Kane et al., 2001; Mozurkewich and Calvert, 1988). The dependence of $\gamma(N_2O_5)$ on RH observed in this study is largely consistent with that observed in Hu and Abbatt, Hallquist et al. and Mozurkewich and Calvert, where $\gamma(N_2O_5)$ is observed to be largely insensitive to RH above 50%. However, our data are in contrast to the results of Kane et al., who observed $\gamma(N_2O_5)$ to increase strongly with RH above 50% RH, which would imply that N_2O_5 hydrolysis is always limited by H_2O(l).

3.2 Dependence of $\gamma(N_2O_5)$ on NO_3^-

We investigated the dependence of $\gamma(N_2O_5)$ on particulate NO_3^- using both aqueous NH_4HSO_4 and malonic acid particles under low and high H_2O(l). To our knowledge, the nitrate effect on multiple particle types has not been directly probed with the same apparatus before. We describe the nitrate effect at $[H_2O(l)] > 15$ M, i.e. above the water limitation

Table 1. Relative humidity, atomizer solution concentrations and mean measured and parameterized reaction probabilities for each experimental condition. The uncertainty in $\gamma(N_2O_5)_{measured}$ is represented as the standard deviation in the measured mean. The uncertainty in $\gamma(N_2O_5)_{parameterized}$ is the propagated uncertainty in Eq. (9).

RH (%)	NH_4HSO_4 (wt %)	Malonic Acid (wt %)	$NaNO_3$ (wt %)	NaCl (wt %)	$\gamma_{meas} \pm 1\sigma$	γ_{param}
60	0.086	0.000	0.000	0.000	0.028±0.006	0.035±0.014
60	0.075	0.000	0.009	0.000	0.025±0.005	0.023±0.010
60	0.065	0.000	0.017	0.000	0.018±0.004	0.017±0.007
60	0.051	0.000	0.026	0.000	0.012±0.003	0.013±0.005
60	0.041	0.000	0.031	0.000	0.009±0.003	0.011±0.004
60	0.028	0.000	0.043	0.000	0.006±0.003	0.008±0.003
60	0.000	0.078	0.000	0.000	0.033±0.006	0.034±0.014
60	0.000	0.071	0.007	0.000	0.024±0.005	0.020±0.009
60	0.000	0.061	0.012	0.000	0.022±0.004	0.015±0.007
60	0.000	0.053	0.021	0.000	0.010±0.003	0.011±0.005
60	0.000	0.031	0.038	0.000	0.007±0.002	0.008±0.003
30	0.000	0.078	0.000	0.000	0.020±0.005	0.020±0.012
30	0.000	0.074	0.003	0.000	0.013±0.003	0.010±0.006
30	0.000	0.073	0.005	0.000	0.001±0.003	0.008±0.005
25	0.000	0.071	0.006	0.000	0.007±0.002	0.006±0.003
20	0.000	0.068	0.008	0.000	0.003±0.001	0.004±0.002
5	0.060	0.000	0.000	0.000	0.005±0.001	0.003±0.008
10	0.060	0.000	0.000	0.000	0.013±0.002	0.009±0.010
15	0.060	0.000	0.000	0.000	0.016±0.003	0.015±0.012
25	0.060	0.000	0.000	0.000	0.024±0.004	0.027±0.013
40	0.060	0.000	0.000	0.000	0.028±0.005	0.033±0.014
50	0.060	0.000	0.000	0.000	0.025±0.004	0.034±0.014
50	0.060	0.000	0.000	0.000	0.026±0.005	0.034±0.014
65	0.060	0.000	0.000	0.000	0.033±0.007	0.035±0.015
75	0.060	0.000	0.000	0.000	0.029±0.007	0.035±0.015
55	0.000	0.000	0.060	0.000	0.001±0.002	0.005±0.002
55	0.000	0.000	0.059	0.001	0.020±0.004	0.017±0.006
55	0.000	0.000	0.058	0.003	0.022±0.005	0.024±0.007
55	0.000	0.000	0.055	0.005	0.026±0.005	0.029±0.008
55	0.000	0.000	0.050	0.010	0.031±0.007	0.032±0.009
55	0.000	0.000	0.000	0.075	0.035±0.007	0.037±0.010

discussed in Sect. 3.1. In these studies, we fixed the RH at 60% and varied the concentration of $NaNO_3$, and either NH_4HSO_4 or malonic acid in the atomizer solution to achieve a range of $[NO_3^-]$ in the particle phase. Atomizer solutions were made at similar total solute wt % to preserve the mean particle size, and a constant RH of 60% ensured that $[H_2O(l)]$ exceeded 20M for the mixed solutions. As depicted in Fig. 3a, $\gamma(N_2O_5)$ decays from a value of 0.03 at $[NO_3^-] = 0$ to less than 0.01 at $[NO_3^-] > 5$ M. In a second set of experiments, we tested the dependence of $\gamma(N_2O_5)$ on NO_3^- at low water (7 M<$[H_2O(l)]$<9M). The results of these experiments, shown as gray squares in Fig. 3a, indicate that the nitrate effect is present at low $H_2O(l)$ and that the two limitations are additive given that the suppression in $\gamma(N_2O_5)$ by nitrate proceeds monotonically from the already suppressed $\gamma(N_2O_5)$ value at zero nitrate.

If N_2O_5 heterogeneous hydrolysis proceeds through the reaction mechanism outlined in Sect. 1, we would expect $\gamma(N_2O_5)$ to be best represented as a competition between H_2O and NO_3^- for the reactive intermediate $H_2ONO_2^+$. This notion is supported by the data shown in Fig. 3b, where $\gamma(N_2O_5)$ is normalized to the value recorded at $[NO_3^-] = 0$ and plotted as a function of the molar ratio of $H_2O(l)$ to NO_3^-. Without normalization the dependence of $\gamma(N_2O_5)$ on $n(H_2O(l))/n(NO_3^-)$ falls along unique "hydropleths" due to the H_2O limitation described in Sect. 3.2. As suggested by Griffiths et al. (2009) the functional form of the normalized curve is determined by the aqueous phase rate coefficients for the reaction of $H_2ONO_2^+$ with $H_2O(l)$ and NO_3^- (Griffiths et al., 2009). While there is no direct experimental evidence for these elementary reactions or the rate coefficients that govern their transformation, we provide empirical constraints on their relative rates in Sect. 4 and compare those constraints with other empirical approaches found in the literature.

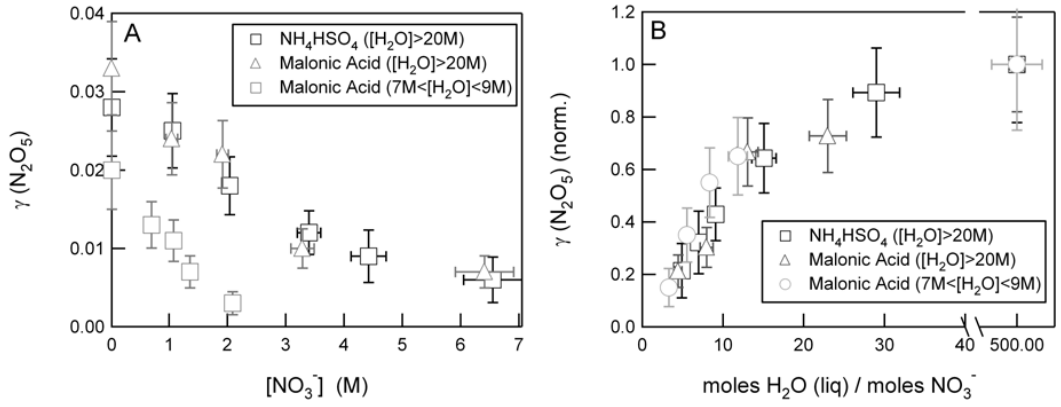

Fig. 3. Dependence of $\gamma(N_2O_5)$ on particle nitrate **(A)** and the molar ratio of particle H_2O to NO_3^- **(B)**. Measurements were made on aqueous NH_4HSO_4 at high H_2O(l) (black squares) and on aqueous malonic acid at both high and low H_2O(l) (gray triangles and circles). Each individual point represents the mean of five independent measurements and the error depicts the standard deviation in the mean. The x-axis error-bars in both panels were calculated in the same methods as described for Fig. 2.

Mentel et al. (1999) and Wahner et al. (1998) first showed that increasing particulate NO_3^- acts to suppress $\gamma(N_2O_5)$ by an order of magnitude for 0 M<[NO_3^-] <27.5 M. In these experiments, variations in the aqueous concentration of NO_3^- were achieved by changing the RH, and thus H_2O(l), resulting in a corresponding change in NO_3^- molarity. These studies and more recent analyses (Griffiths et al., 2009) assumed there was no dependence of $\gamma(N_2O_5)$ on H_2O(l) for aqueous particles. In our study, we treat the H_2O(l) and NO_3^- dependencies independently, with the objective of determining a combined function for $\gamma(N_2O_5)$ that incorporates both of these effects.

3.3 Dependence of $\gamma(N_2O_5)$ on Cl^-

As outlined in Sect. 1, any available aqueous phase nucleophile can compete for the $H_2ONO_2^+$ reaction intermediate, thus altering the net reactivity. N_2O_5 hydrolysis on aqueous particles containing chloride has been observed to be rapid ($\gamma(N_2O_5) = 0.03$) (Behnke et al., 1997; Thornton and Abbatt, 2005), and measurement of the nitryl chloride ($ClNO_2$) product yields (100% at [Cl^-] > 4 M) confirm that the reaction proceeds through Reaction (R4) when sufficient [Cl^-] exists in the condensed phase (Behnke et al., 1997; Thornton and Abbatt, 2005). To the best of our knowledge, the competition of Cl^- and NO_3^- for $H_2ONO_2^+$ has not been investigated. The relative reactivity of Cl^- and H_2O, implied by Behnke et al. (1997), suggest that trace Cl^- may negate the nitrate effect in many parts of the atmosphere where Cl^- and NO_3^- are internally mixed within a particle population (Behnke et al., 1997). Here, we investigate this conjecture using mixed NaCl-$NaNO_3$ particles at high H_2O(l).

In this set of experiments, we fixed the RH at 55% and varied the concentration of $NaNO_3$and NaCl in the atomizer solution to achieve a range in [Cl^-], while maintaining high NO_3^- ([NO_3^-]>10M) and H_2O(l) ([H_2O(l)] > 20 M). As a result, the experiment is designed to directly probe the competition between NO_3^- and Cl^- for the reaction intermediate, $H_2ONO_2^+$. As depicted in Fig. 4a, $\gamma(N_2O_5)$ is suppressed at low [Cl^-] due to high [NO_3^-], but increases sharply with increasing [Cl^-]. For a [Cl^-] as low as 2 M, reaction 4 entirely negates the nitrate effect. Our rate determinations are corroborated by analysis of the reaction products. Direct measure of the $ClNO_2$ reaction product confirms reaction R4 occurred in these mixed composition particles. This result is shown in Fig. 4b, where the product yield ($Y_{ClNO_2} = \Delta ClNO_2/\Delta N_2O_5$) approaches unity as [$Cl^-$] approaches 1 M. The observed product yield is consistent with the results of Behnke et al. to within the combined uncertainty of the two experiments (Behnke et al., 1997).

4 Generalized parameterization of $\gamma(N_2O_5)$

We use the laboratory results described in Sect. 3 to generate a general parameterization for the heterogeneous hydrolysis of N_2O_5 that includes the dependence of $\gamma(N_2O_5)$ on [H_2O](l), [NO_3^-], and [Cl^-]. The parameterization described here assumes that the particle population is internally mixed and that reactions are permitted to occur throughout the particle volume without diffusive limitations. These assumptions, alongside additional dependencies suggested in the literature are discussed in Sect. 4.3.

We follow the framework designed by Wahner et al. (1998) and Griffiths et al. (2009) to assess the relative effects of the dependence of $\gamma(N_2O_5)$ on H_2O(l) and NO_3^- and Cl^- molarity (Griffiths et al., 2009; Wahner et al., 1998). By assuming that the solvated NO_2^+ intermediate ($H_2ONO_2^+$) is in steady-state, an expression for $\gamma(N_2O_5)$ can be derived in terms of H_2O(l), NO_3^-, Cl^-, and the rate coefficients for

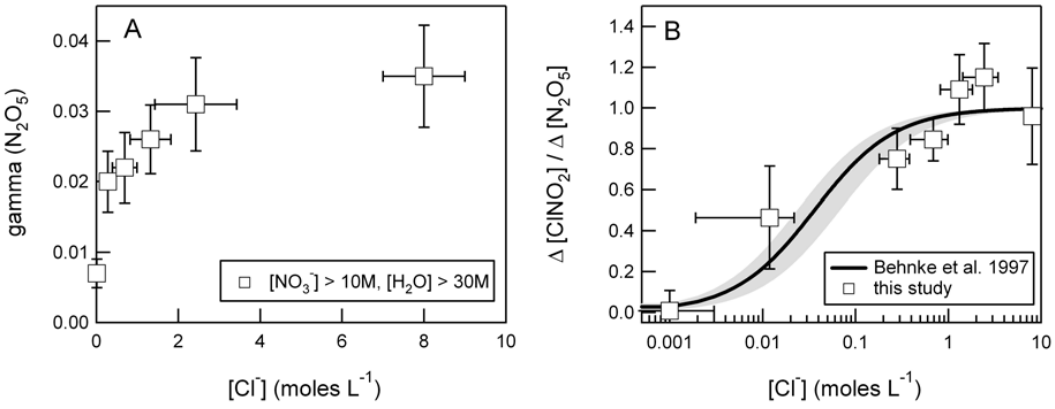

Fig. 4. Dependence of $\gamma(N_2O_5)$ on particle chloride **(A)** and the yield of $ClNO_2$ resulting from N_2O_5 hydrolysis **(B)**. Measurements were made on mixed aqueous $NaNO_3$/NaCl particles at high H_2O(l) and high NO_3^-. In panel B, the yield curve determined by Behnke et al. (1997), is included for comparison (1997). Again, each individual point represents the mean of five independent measurements and the error depicts the standard deviation in the mean. The x-axis error-bars in both panels were calculated in the same methods as described for Fig. 2.

Reactions (R1–4), as shown in Eq. (3–9). Here we assume that the reaction is volume limited, and that N_2O_5(g) and N_2O_5(aq) have reached Henry's law equilibrium. We then solve for the net reactivity of N_2O_5(aq) (E3). The rate coefficients for Reactions (R1–4) are represented as k_1-k_4 below, where the subscripts f and r correspond to the forward and reverse reactions, respectively.

$$\frac{d[N_2O_5(aq)]}{dt} = k_{2b}\left[H_2ONO_2^+\right]\left[NO_3^-\right] - k_{2f}[N_2O_5(aq)][H_2O(l)] \quad (3)$$

$$\frac{d\left[H_2ONO_2^+\right]}{dt} = k_{2f}[N_2O_5(aq)][H_2O(l)] - k_{2b}\left[H_2ONO_2^+\right]\left[NO_3^-\right] - k_3\left[H_2ONO_2^+\right][H_2O(l)] - k_4\left[H_2ONO_2^+\right]\left[Cl^-\right] = 0 \quad (4)$$

$$\left[H_2ONO_2^+\right] = \frac{k_{2f}[N_2O_5(aq)][H_2O(l)]}{k_3[H_2O(l)] + k_{2b}\left[NO_3^-\right] + k_4\left[Cl^-\right]} \quad (5)$$

Substitution of Eq (5) into Eq (3) yields,

$$\frac{d[N_2O_5(aq)]}{dt} = \frac{k_{2b}\left[NO_3^-\right]k_{2f}[N_2O_5(aq)][H_2O(l)]}{k_3[H_2O(l)] + k_{2b}\left[NO_3^-\right] + k_4\left[Cl^-\right]} - k_{2f}[N_2O_5(aq)][H_2O(l)] \quad (6)$$

Assuming that N_2O_5 mass accommodation (α) proceeds with high efficiency and that the liquid-phase reactions occur throughout the entire particle volume, we can derive an expression for $\gamma(N_2O_5)$.

$$\gamma_{N_2O_5} = \frac{4L_{N_2O_5(aq)}V}{\omega S_a[N_2O_5(g)]}, \quad (7)$$

where $L_{N_2O_5(aq)} = -\frac{d[N_2O_5(aq)]}{dt}$

$$\gamma_{N_2O_5} = \frac{4k_{2f}[N_2O_5(aq)][H_2O(l)]\left(1 - \frac{k_{2b}[NO_3^-]}{k_3[H_2O(l)] + k_{2b}[NO_3^-] + k_4[Cl^-]}\right)V}{\omega S_a[N_2O_5(g)]} \quad (8)$$

$$\gamma_{N_2O_5} = \frac{4}{\omega}\frac{V}{S_a}K_H k'_{2f}\left(1 - \frac{1}{\left(\frac{k_3[H_2O(l)]}{k_{2b}[NO_3^-]}\right) + 1 + \left(\frac{k_4[Cl^-]}{k_{2b}[NO_3^-]}\right)}\right) \quad (9)$$

In Eqs. (7–9), V is the total particle volume concentration ($m^3\,m^{-3}$), S_a is the total particle surface area concentration ($m^2\,m^{-3}$), ω is the mean molecular speed of N_2O_5 ($m\,s^{-1}$) and K_H is the dimensionless Henry's law coefficient ($K_H \equiv [N_2O_5]_{aq}/[N_2O_5]_g$). In Eq. (9), we treat the rate coefficient for $R2_f$ to be a function of H_2O(l) in order to account for the H_2O-limitation observed in the nitrate-free particles and redefine it as k'_{2f}.

As illustrated by Eq. (9), $\gamma(N_2O_5)$ is a function of H_2O(l), NO_3^-, and Cl^-; the relative importance of each set by the rate coefficients depicted in Reactions (1–4). As noted by Wahner et al. (1998), quantitative calculation of $\gamma(N_2O_5)$ is limited by large uncertainty in $K_H(N_2O_5)$, the rate coefficients k_{2b}, k_{2f}, k_3, and k_4, and assumptions concerning concentrated and supersaturated solutions. Further, in the event that the

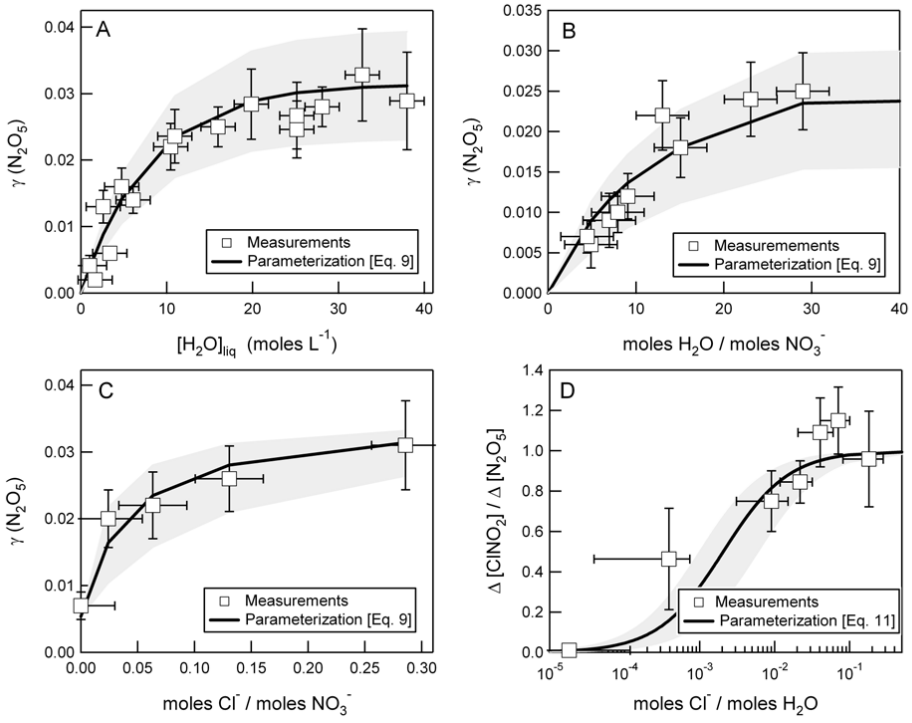

Fig. 5. Laboratory observations of the dependence of $\gamma(N_2O_5)$ on particle H_2O(l) **(A)**, the molar ratio of H_2O(l)/NO_3^- **(B)** and the molar ratio of Cl^-/NO_3^- (black squares). The uncertainty-weighted least squares fit for each (as described in Sect. 4.1) are included in panels **(A–C)** (solid lines) alongside the uncertainty associated with the fit parameters (shaded region). Panel **(D)** depicts the measured $ClNO_2$ product yield as a function of the molar ratio of Cl^-/NO_3^- (black squares). The solid line corresponds to the yield calculated using Eq. (11).

diffusion of N_2O_5 through the particle is slower than its reaction, $\gamma(N_2O_5)$ will be a function of the liquid-phase diffusion rates. Empirical limits have been placed on several of the rate coefficients and equilibrium constants, permitting qualitative evaluation of the solution-phase functional dependences of $\gamma(N_2O_5)$ (Behnke et al., 1997; Griffiths et al., 2009; Mentel et al., 1999; Wahner et al., 1998). In the following discussion, we use the results described in Sect. 3 to provide a new set of constraints for Eq. (9) that capture the simultaneous dependence of $\gamma(N_2O_5)$ on H_2O(l), NO_3^- and Cl^-.

4.1 Empirical constraints on aqueous phase rate coefficients

The application of Eq. (9) to determine $\gamma(N_2O_5)$ requires accurate representation of both the dissociation rate of N_2O_5(aq), k'_{2f} and the relative rates for the two competing reactions (k_3/k_{2b} and k_4/k_{2b}) involving the intermediate. The experiments we present herein were designed to allow for independent assessment of each of the rate terms shown in Eq. (9). In this analysis, we take K_H (N_2O_5) as 51 (Fried et al., 1994) and $V \times S_a^{-1}$ as 3.75×10^{-8} m, which is the mean value measured in our experiments.

To derive quantitative estimates of the reaction rate coefficients for $R2_f$, and for the ratios k_3/k_{2b} and k_4/k_{2b}, we first use the results of the H_2O(l) (Sect. 3.1) study to isolate the effect of H_2O(l) which we presume is the strongest in $R2_f$. Using an uncertainty-weighted least squares fit, we find k'_{2f} to be best captured as,

$$k'_{2f} = \beta - \beta e^{(-\delta[H_2O(l)])} \quad (10)$$

where β as determined to be $1.15 \times 10^6 \pm 3 \times 10^5\ s^{-1}$ and δ determined to be $1.3 \times 10^{-1} \pm 5 \times 10^{-2}\ M^{-1}$ (Fig. 5a). It is important to note that in this representation, a solid particle, by definition would have zero H_2O(l), and k'_{2f} would be set to zero. This results in $\gamma(N_2O_5)$ equal to zero for solid particles. Non-zero values for $\gamma(N_2O_5)$ have been observed in the laboratory on solid particles (Hallquist et al., 2003; Kane et al., 2001; Mozurkewich and Calvert, 1988), and thus our parameterization is only valid for the aqueous volume present in a particle population.

We then constrain k'_{2f} by Eq. (10) and use a separate uncertainty-weighted least squares fit to determine k_3/k_{2f} for the nitrate experiments described in Sect. 3.2 (Fig. 5b). Our experimental value of $6.0 \times 10^{-2} \pm 1.0 \times 10^{-2}$ is in reasonably good agreement with the recent work of Griffiths et al. (2009), where they determined k_3/k_{2f} to be 3.3×10^{-2}. Finally, holding both k'_{2f} and k_3/k_{2f} to the values resulting from their respective fits, we calculate k_4/k_{2b} from our

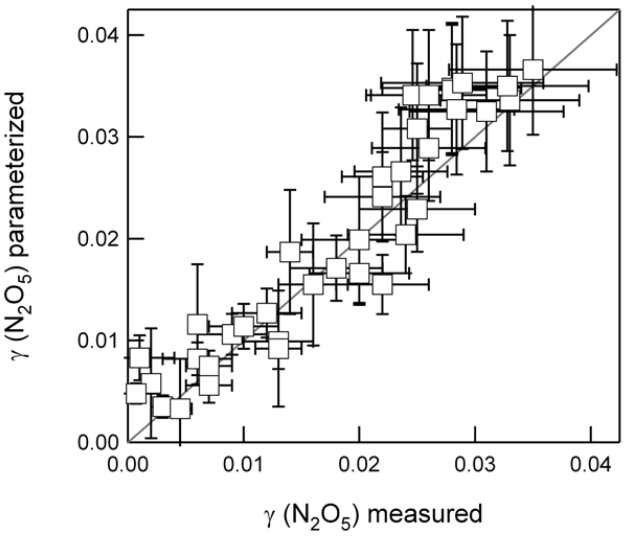

Fig. 6. Comparison of laboratory measured $\gamma(N_2O_5)$ with that parameterized using Eq. (9) for all 39 sets of observations. Each individual point represents the mean of five independent measurements and the error-bar in $\gamma(N_2O_5)_{measured}$ depicts the standard deviation in the measured mean. The error-bar in $\gamma(N_2O_5)_{parameterized}$ is the propagated uncertainty in Eq. (9).

Table 2. Fitting parameters calculated for use in Eq. (10) and (12).

Parameter	Value
A [s]	3.2×10^{-8}
β [s^{-1}]	$1.15\times10^{6}\pm3\times10^{5}$
δ [M^{-1}]	$1.3\times10^{-1}\pm5\times10^{-2}$
k_3/k_{2b}	$6.0\times10^{-2}\pm1.0\times10^{-2}$
k_4/k_{2b}	29 ± 6

chloride experiments (Sect. 3.3, Fig. 5c). The values and their associated uncertainties, derived from the uncertainty-weighted least squares fits, are summarized in Table 2. In Fig. 6, all 38 laboratory determinations of $\gamma(N_2O_5)$ are compared with that predicted using Eq. (9) for each individual set of conditions. The strong agreement over a wide range of H_2O(l), NO_3^-, and Cl^- suggests that this parameterization will be useful for assessing the competing effects of H_2O, NO_3^-, and Cl^- in internally mixed atmospheric particles.

An additional test of the above fit parameters is the prediction of the observed product yield for $ClNO_2$ (Y_{ClNO_2}). Y_{ClNO_2} was directly measured during in the chloride experiments and can be calculated as,

$$Y_{ClNO_2} = \frac{\Delta ClNO_2}{\Delta N_2O_5} = \left(1 + \frac{k_3\,[H_2O(l)]}{k_4\,[Cl^-]}\right)^{-1} \quad (11)$$

Where the value for k_4/k_3 ($k_4/k_3 = 483\pm175$) is taken from the above determinations of k_3/k_{2f} and k_4/k_{2f}. As depicted in Fig. 5d, our results agree to within the combined uncertainty of the two determinations. Our determination of k_4/k_3 is smaller than that inferred from the results of Behnke et al. (1997) ($k_4/k_3 = 836\pm32$) .

4.2 Validity of the current parameterization

The validity of the current parameterization for use in atmospheric models ultimately depends on the validity of the assumptions made to derive it. We discuss some of these issues further here. First, as mentioned above, the parameterization is designed to address an internally mixed particle population. Ambient observations of particle mixing state suggest that particles are predominately internally mixed outside of the immediate source region (Murphy et al., 2006). It is important to note that Eq. (9) can be applied to an externally mixed particle population, if the composition and relative contributions of the different particle types to the total surface area are known. However, if a particle population is internally mixed in reality, but it is treated as externally mixed, then applying the above parameterization will likely lead to unrealistic $\gamma(N_2O_5)$ values. Our laboratory results show that $\gamma(N_2O_5)$ depends on the internal mixing of water, nitrate and chloride, and thus highlight the need for in situ observations of particle mixing state to ultimately test and understand N_2O_5 reactivity on atmospheric aerosol particles.

Second, the above parameterization does not include the effects of films. Organic films have been shown in the laboratory to suppress $\gamma(N_2O_5)$ (Badger et al., 2006; Cosman and Bertram, 2008; Cosman et al., 2008; Folkers et al., 2003; McNeill et al., 2006; Park et al., 2007). The measured suppression has been postulated to be a result of a decrease in: i) the N_2O_5 mass accommodation coefficient, ii) the availability of H_2O(l), or iii) the aqueous phase diffusion constant for N_2O_5 (Anttila et al., 2006). However, despite the extensive laboratory characterization, to the best of our knowledge, ambient observations of organic films are lacking.

Third, we have assumed that reactions can occur throughout the entire particle volume. The reaction may be confined to a surface layer due to an aqueous phase diffusion limitation for N_2O_5 (Griffiths et al., 2009, Wahner et al., 1998). This limitation has been accounted for in several analyses by invoking a reacto-diffusion length. We also attempted to parameterize our results in this fashion, however least squares fits to the diffusion limited formula, analogous to Eq. (9), did not yield statistically different results, and in fact produced worse agreement in the data. For this reason we have not included the diffusion limitation, especially given the uncertainty in the aqueous phase diffusion coefficient for N_2O_5 in the highly ionic and non-ideal solutions used here. Given that the particle sizes used in our experiments are similar to those that contain most of the surface area in polluted environments, we feel this choice will not greatly affect the application of Eq. (9) to most atmospheric conditions.

Finally, crystalline or largely solid particles, such as effloresced sea spray or mineral dust, and the role of temperature have not been included in this parameterization. Recent laboratory investigations have shown that N_2O_5 proceeds moderately efficiently on dust particles, $\gamma(N_2O_5) = 0.013 \pm 0.002$ (Wagner et al., 2008). Our parameterization would not capture these values, though the amount of liquid water and the true surface area-to-volume ratio would be required for a direct comparison. Thus, we recommend against applying this parameterization where dust contributes significantly to the available particle surface area. Hallquist et al. (2003) have shown a strong temperature dependence in the heterogeneous reaction, where $\gamma(N_2O_5)$ on NH_4HSO_4 particles at 50% RH ranged between 0.03 and 0.003 for a temperature between 263 and 308 K (2003). However, Schweitzer et al., showed little to no temperature dependence for halide salt solutions (Schweitzer et al., 1998). As a result, we stress that our parameterization has been determined for an average temperature of 298K, but could include a T-dependence when it is known whether that dependence occurs in the reaction of N_2O_5 on aqueous solution particles.

4.3 Comparison to existing model parameterizations of $\gamma(N_2O_5)$

The impact of N_2O_5 heterogeneous reactions on global tropospheric NO_x and O_3 was first explored by Dentener and Crutzen, where they employed a globally uniform $\gamma(N_2O_5)$ of 0.1, based upon laboratory studies conducted under conditions most relevant to the stratosphere (Dentener and Crutzen, 1993). These results indicated that accurate representation of the heterogeneous hydrolysis of N_2O_5 was critical for understanding both NO_x loadings and O_3 production rates in the troposphere. It was not until recently that tropospheric model parameterizations of $\gamma(N_2O_5)$ have been revisited. These efforts have largely been in response to a growing number of laboratory experiments designed to elucidate the functional dependencies of $\gamma(N_2O_5)$ on tropopspheric particles, which display strong heterogeneity in chemical composition and liquid water content, and to field observations which infer a spatially and temporally varying N_2O_5 reactivity which correlates with changes in particle composition and humidity changes.

A variety of parameterizations have been developed. Riemer et al. (2003) implemented a parameterization that differentiated between nitrate and sulfate particles, prescribing values of 0.02 and 0.002 for $\gamma(N_2O_5)$, respectively (Riemer et al., 2003). Evans and Jacob expanded beyond this, treating $\gamma(N_2O_5)$ as a function of an external mixture of a wide range of chemical constituents (e.g., sulfate, organic and black carbon, dust and sea salt) and included both a temperature and RH dependence. In the Evans and Jacob analysis: i) the organic mass fraction is treated as malonic acid (a highly soluble dicarboxylic acid), ii) $\gamma(N_2O_5)$ is allowed to increase strongly with RH for RH>50% on ammonium sulfate particles, which is inconsistent with our present results and those of others (Hallquist et al., 2003; Mozurkewich and Calvert, 1988), and iii) the nitrate effect is not included (Evans and Jacob, 2005). Most recently, Davis et al. published a parameterization that includes the effects of nitrate, sulfate, temperature, RH and particle phase (Davis et al., 2008), while Riemer et al. (2009) have extended their parameterization to include the effects of organic coatings.

Our parameterization is unique in that it is driven by the fundamental chemical properties that control $\gamma(N_2O_5)$ on aqueous solution particles, namely particle H_2O(l), NO_3^- and Cl^-. It has been formulated in a way that can be coupled directly to an aerosol thermodynamic model (e.g., AIM, ISOROPIA, and MOSAIC) and can be implemented for either internal or externally mixed particles (Clegg et al., 1998; Fountoukis and Nenes, 2007; Zaveri et al., 2008). As a result, advances in the representation of particle H_2O(l) will directly translate into improvements into the treatment of $\gamma(N_2O_5)$. This aspect is particularly important in the area of organic carbon, where the dependence of H_2O(l) on organic composition and loading for RH<95% remains poorly quantified (Quinn et al., 2005).

5 Conclusions

We report laboratory measurements of the dependence of $\gamma(N_2O_5)$ on particle H_2O(l), NO_3^- and Cl^-, conducted using internally mixed aqueous inorganic and organic particles. The novel measurements show a strong dependence of $\gamma(N_2O_5)$ on H_2O(l) below 15M and illustrate the competition of H_2O(l), NO_3^-, and Cl^- for the $H_2ONO_2^+$ reaction intermediate. The effect of H_2O(l) will not only depend on RH but also on the hygroscopicity of the particle components. We confirm that nitrate can suppress $\gamma(N_2O_5)$ at H_2O(l) to NO_3^- molar ratios below 20, and illustrate through measurements of both $\gamma(N_2O_5)$ and Y_{ClNO_2}, that trace Cl^- can negate the nitrate effect at Cl^- to NO_3^- molar ratios greater than 0.1.

Based on the aforementioned laboratory experiments, we suggest that $\gamma(N_2O_5)$ can be parameterized within regional or global chemical transport models as:

$$\gamma_{N_2O_5} = A k_{2f}^{'} \left(1 - \frac{1}{\left(\frac{k_3[H_2O(l)]}{k_{2b}[NO_3^-]}\right) + 1 + \left(\frac{k_4[Cl^-]}{k_{2b}[NO_3^-]}\right)} \right) \quad (12)$$

where A (3.2×10^{-8} s) is an empirical pre-factor that includes V, S_a, ωs and K_H, and $k_{2f}^{'}$ is calculated using E10. The parameterization as developed is meant to be driven by a coupled aerosol thermodynamics model to generate the aqueous phase concentrations required for calculation of $\gamma(N_2O_5)$.

Further, the parameterization can be used to directly test ambient observations of $\gamma(N_2O_5)$ (Bertram et al., 2009) or the steady-state lifetimes of N_2O_5 (Brown et al., 2006).

Acknowledgements. THB gratefully acknowledges the NOAA Climate and Global Change Fellowship Program for financial support. We thank Sihem Ben Abdelmelek and Dean Hegg for assistance with the IC analysis of the atomizer solutions.

Edited by: J. B. Burkholder

References

Anttila, T., Kiendler-Scharr, A., Tillmann, R., and Mentel, T. F.: On the reactive uptake of gaseous compounds by organic-coated aqueous aerosols: Theoretical analysis and application to the heterogeneous hydrolysis of N_2O_5, J. Phys. Chem. A, 110, 10435–10443, 2006.

Badger, C. L., Griffiths, P. T., George, I., Abbatt, J. P. D., and Cox, R. A.: Reactive uptake of N_2O_5 by aerosol particles containing mixtures of humic acid and ammonium sulfate, J. Phys. Chem. A, 110, 6986-6994, 2006.

Behnke, W., George, C., Scheer, V., and Zetzsch, C.: Production and decay of $ClNO_2$, from the reaction of gaseous N_2O_5 with NaCl solution: Bulk and aerosol experiments, J. Geophys. Res., 102, 3795–3804, 1997.

Bertram, T. H., Thornton, J. A. and Riedel, T. P.: An experimental technique for the direct measurement of N_2O_5 reactivity on ambient particles, Atmos. Meas. Tech., 2, 231–242, 2009, http://www.atmos-meas-tech.net/2/231/2009/.

Braban, C. F. and Abbatt, J. P. D.: A study of the phase transition behavior of internally mixed ammonium sulfate-malonic acid aerosols, Atmos. Chem. Phys., 4, 1451–1459, 2004, http://www.atmos-chem-phys.net/4/1451/2004/.

Brown, R. L.: Tubular Flow Reactors with 1st-Order Kinetics, J. Res. Nat. Bureau Stand., 83, 1–8, 1978.

Brown, S. S., Ryerson, T. B., Wollny, A. G., Brock, C. A., Peltier, R., Sullivan, A. P., Weber, R. J., Dube, W. P., Trainer, M., Meagher, J. F., Fehsenfeld, F. C., and Ravishankara, A. R.: Variability in nocturnal nitrogen oxide processing and its role in regional air quality, Science, 311, 67–70, 2006.

Carslaw, K. S., Clegg, S. L., and Brimblecombe, P.: A Thermodynamic Model of the System HCl-HNO_3-H_2SO_4-H_2O, Including Solubilities of HBr, from Less Than 200 to 328 K, J. Phys. Chem., 99, 11557–11574, 1995.

Clegg, S. L., Brimblecombe, P., and Wexler, A. S.: Thermodynamic model of the system H^+-NH_4^+-Na^+-SO_4^{2-}-NO_3^--Cl^--H_2O at 298.15 K, J. Phys. Chem. A, 102, 2155–2171, 1998.

Cosman, L. M. and Bertram, A. K.: Reactive uptake of N_2O_5 on aqueous H_2SO_4 solutions coated with 1-component and 2-component monolayers, J. Phys. Chem. A, 112, 4625–4635, 2008.

Cosman, L. M., Knopf, D. A., and Bertram, A. K.: N_2O_5 reactive uptake on aqueous sulfuric acid solutions coated with branched and straight-chain insoluble organic surfactants, J. Phys. Chem. A, 112, 2386–2396, 2008.

Cziczo, D. J., Nowak, J. B., Hu, J. H., and Abbatt, J. P. D.: Infrared spectroscopy of model tropospheric aerosols as a function of relative humidity: Observation of deliquescence and crystallization, J. Geophys. Res., 102, 18843–18850, 1997.

Davis, J. M., Bhave, P. V., and Foley, K. M.: Parameterization of N2O5 reaction probabilities on the surface of particles containing ammonium, sulfate, and nitrate, Atmos. Chem. Phys., 8, 5295–5311, 2008, http://www.atmos-chem-phys.net/8/5295/2008/.

Dentener, F. J. and Crutzen, P. J.: Reaction of N_2O_5 on tropospheric aerosols - Impact on the global distributions of NO_x, O_3, and OH, J. Geophys. Res., 98, 7149–7163, 1993.

Evans, M. J. and Jacob, D. J.: Impact of new laboratory studies of N_2O_5 hydrolysis on global model budgets of tropospheric nitrogen oxides, ozone, and OH, Geophys. Res. Lett., 32, L09813, doi:10.1029/2005GL022469, 2005.

Finlayson-Pitts, B. J., Ezell, M. J., and Pitts, J. N.: Formation of chemically active chlorine compounds by reactions of atmospheric NaCl particles with gaseous N_2O_5 and $ClONO_2$, Nature, 337, 241–244, 1989.

Folkers, M., Mentel, T. F., and Wahner, A.: Influence of an organic coating on the reactivity of aqueous aerosols probed by the heterogeneous hydrolysis of N_2O_5, Geophys. Res. Lett., 30(12), 1644, doi:10.1029/2003GL017168, 2003.

Fountoukis, C. and Nenes, A.: ISORROPIA II: a computationally efficient thermodynamic equilibrium model for K + -Ca_2 + -Mg_2 + -Nh(4)(+)-Na + -SO_4^{2}–NO_3–Cl–H_2O aerosols, Atmos. Chem. Phys., 7, 4639–4659, 2007, http://www.atmos-chem-phys.net/7/4639/2007/.

Fried, A., Henry, B. E., Calvert, J. G., and Mozurkewich, M.: The reaction probability of N_2O_5 with sulfuric-acid aerosols at stratospheric temperatures and compositions, J. Geophys. Res., 99, 3517–3532, 1994.

Griffiths, P. T., Badger, C. L., Cox, R. A., Folkers, M., Henk, H. H., and Mentel, T. F.: Reactive Uptake of N2O5 by Aerosols Containing Dicarboxylic Acids. Effect of Particle Phase, Composition, and Nitrate Content, J. Phys. Chem. A, 113, 5082–5090, 2009.

Hallquist, M., Stewart, D. J., Stephenson, S. K., and Cox, R. A.: Hydrolysis of N2O5 on sub-micron sulfate aerosols, PCCP, 5, 3453–3463, 2003.

Hanson, D. and Kosciuch, E.: The NH_3 mass accommodation coefficient for uptake onto sulfuric acid solutions, J. Phys. Chem. A, 107, 2199–2208, 2003.

Hu, J. H. and Abbatt, J. P. D.: Reaction probabilities for N_2O_5 hydrolysis on sulfuric acid and ammonium sulfate aerosols at room temperature, J. Phys. Chem. A, 101, 871–878, 1997.

Kane, S. M., Caloz, F. and Leu, M. T.: Heterogeneous uptake of gaseous N2O5 by (NH4)(2)SO4, NH4HSO4, and H2SO4 aerosols, J. Phys. Chem. A, 105, 6465–6470, 2001.

Kercher, J. P., Reidel, T., and Thornton, J. A.: Chlorine activation by N_2O_5: In situ detection of $ClNO_2$ and N_2O_5 by chemical ionization mass spectrometry, Atmos. Meas. Tech., 2, 193–204, 2009, http://www.atmos-meas-tech.net/2/193/2009/.

Knopf, D. A., Cosman, L. M., Mousavi, P., Mokamati, S., and Bertram, A. K.: A novel flow reactor for studying reactions on liquid surfaces coated by organic monolayers: Methods, validation, and initial results, J. Phys. Chem. A, 111, 11021–11032, 2007.

McNeill, V. F., Patterson, J., Wolfe, G. M., and Thornton, J. A.: The effect of varying levels of surfactant on the reactive uptake of N_2O_5 to aqueous aerosol, Atmos. Chem. Phys., 6, 1635–1644,

2006, http://www.atmos-chem-phys.net/6/1635/2006/.

Mentel, T. F., Sohn, M., and Wahner, A.: Nitrate effect in the heterogeneous hydrolysis of dinitrogen pentoxide on aqueous aerosols, PCCP, 1, 5451–5457, 1999.

Mozurkewich, M. and Calvert, J. G.: Reaction probability of N_2O_5 on aqueous aerosols, J. Geophys. Res., 93, 15889–15896, 1988.

Murphy, D. M., Cziczo, D. J., Froyd, K. D., Hudson, P. K., Matthew, B. M., Middlebrook, A. M., Peltier, R. E., Sullivan, A., Thomson, D. S. and Weber, R. J.: Single-particle mass spectrometry of tropospheric aerosol particles, J. Geophys. Res., 111, D23S32, doi:10.1029/2006JD007340, 2006.

Osthoff, H. D., Roberts, J. M., Ravishankara, A. R., Williams, E. J., Lerner, B. M., Sommariva, R., Bates, T. S., Coffman, D., Quinn, P. K., Dibb, J. E., Stark, H., Burkholder, J. B., Talukdar, R. K., Meagher, J., Fehsenfeld, F. C., and Brown, S. S.: High levels of nitryl chloride in the polluted subtropical marine boundary layer, Nature Geoscience, 1, 324–328, 2008.

Park, S. C., Burden, D. K., and Nathanson, G. M.: The inhibition of N_2O_5 hydrolysis in sulfuric acid by 1-butanol and 1-hexanol surfactant coatings, J. Phys. Chem. A, 111, 2921–2929, 2007.

Quinn, P. K., Bates, T. S., Baynard, T., Clarke, A. D., Onasch, T. B., Wang, W., Rood, M. J., Andrews, E., Allan, J., Carrico, C. M., Coffman, D., and Worsnop, D.: Impact of particulate organic matter on the relative humidity dependence of light scattering: A simplified parameterization, Geophys. Res. Lett., 32, L22809, doi:10.1029/2005GL024322, 2005.

Riemer, N., Vogel, H., Vogel, B., Schell, B., Ackermann, I., Kessler, C., and Hass, H.: Impact of the heterogeneous hydrolysis of N_2O_5 on chemistry and nitrate aerosol formation in the lower troposphere under photosmog conditions, J. Geophys. Res., 108(D4), 4144, doi:10.1029/2002JD002436, 2003.

Riemer, N., Vogel, H., Vogel, B., Anttila, T., Kiendler-Scharr, A., and Mentel, T. F.: The relative importance of organic coatings for the heterogeneous hydrolysis of N_2O_5, 114, D17307, doi:10.1029/2008JD011369, 2009.

Robinson, G. N., Worsnop, D. R., Jayne, J. T., Kolb, C. E., and Davidovits, P.: Heterogeneous uptake of $ClONO_2$ and N_2O_5 by sulfuric acid solutions, J. Geophys. Res., 102, 3583–3601, 1997.

Schweitzer, F., Mirabel, P., and George, C.: Multiphase chemistry of N_2O_5, $ClNO_2$, and $BrNO_2$, J. Phys. Chem. A, 102, 3942–3952, 1998.

Thornton, J. A. and Abbatt, J. P. D.: N_2O_5 reaction on submicron sea salt aerosol: Kinetics, products, and the effect of surface active organics, J. Phys. Chem. A, 109, 10004–10012, 2005.

Thornton, J. A., Braban, C. F., and Abbatt, J. P. D.: N_2O_5 hydrolysis on sub-micron organic aerosols: the effect of relative humidity, particle phase, and particle size, PCCP, 5, 4593–4603, 2003.

Wagner, C., Hanisch, F., Holmes, N., de Coninck, H., Schuster, G., and Crowley, J. N.: The interaction of N2O5 with mineral dust: aerosol flow tube and Knudsen reactor studies, Atmos. Chem. Phys., 8, 91–109, 2008, http://www.atmos-chem-phys.net/8/91/2008/.

Wahner, A., Mentel, T. F., Sohn, M. and Stier, J.: Heterogeneous reaction of N_2O_5 on sodium nitrate aerosol, J. Geophys. Res., 103, 31103–31112, 1998.

Wexler, A. S. and Clegg, S. L.: Atmospheric aerosol models for systems including the ions H^+, NH_4^+, Na^+, SO_4^{2-}, NO_3^-,Cl^-, Br^-, and H_2O, J. Geophys. Res., 107(D14), 4207, doi:10.1029/2001JD000451, 2002.

Zaveri, R. A., Easter, R. C., Fast, J. D. and Peters, L. K.: Model for Simulating Aerosol Interactions and Chemistry (MOSAIC), J. Geophys. Res., 113, D13204, doi:10.1029/2007JD008782, 2008.